FEBS Letters

FEBS PRESS science publishing by scientists

An *in vivo* proteomic analysis of the Me31B interactome in *Drosophila* germ granules

Hunter DeHaan[1], Aidan McCambridge[1], Brittany Armstrong[1], Carlie Cruse[1], Dhruv Solanki[1], Jonathan C. Trinidad[2], Alexey L. Arkov[3] and Ming Gao[1]

1 Biology Department, Indiana University Northwest, Gary, IN, USA
2 Department of Chemistry, Indiana University, Bloomington, IN, USA
3 Department of Biological Sciences, Murray State University, Murray, KY, USA

Correspondence
M. Gao, Biology Department, Indiana University Northwest, Marram Hall 310, 3400 Broadway, Gary, IN 46408, USA
Fax: +1 219 980 7125
Tel: +1 219 980 6722
E-mail: minggao@iun.edu

(Received 4 August 2017, revised 7 September 2017, accepted 15 September 2017, available online 11 October 2017)

doi:10.1002/1873-3468.12854

Edited by Didier Stainier

***Drosophila* Me31B is a conserved protein of germ granules, ribonucleoprotein complexes essential for germ cell development. Me31B post-transcriptionally regulates mRNAs by interacting with other germ granule proteins. However, a Me31B interactome is lacking. Here, we use an *in vivo* proteomics approach to show that the Me31B interactome contains polypeptides from four functional groups: RNA regulatory proteins, glycolytic enzymes, cytoskeleton/motor proteins, and germ plasm components. We further show that Me31B likely colocalizes with the germ plasm components Tudor (Tud), Vasa, and Aubergine in the nuage and germ plasm and provide evidence that Me31B may directly bind to Tud in a symmetrically dimethylated arginine-dependent manner. Our study supports the role of Me31B in RNA regulation and suggests its novel roles in germ granule assembly and function.**

Keywords: *Drosophila*; germ cells; germ granules; *in vivo* interactome; Me31B; RNA helicase

Germ granules are cytoplasmic granular particles widely found in germ cells. Germ granule components are essential for the development of the germline and the formation of germ cells, which give rise to gametes and eventually the next generation [1–6]. In the oogenesis of *Drosophila melanogaster*, germ granule components are first synthesized in nurse cells, transported and localized posteriorly to developing oocytes, and form germ plasm there, which in turn dictates the formation of germ cells [1,4,7–10]. During development, these granules are highly dynamic in their subcellular location, morphology, and molecular composition [4,11].

At the molecular level, germ granules are composed of large RNA–protein complexes generally referred to as ribonucleoproteins (RNPs). *Drosophila* Me31B, a DEAD-box ATP-dependent RNA helicase, is a conserved protein component of the germ granule RNPs [12,13]. During oogenesis, Me31B is associated with different forms of germ granules: perinuclear granules (nuage) of nurse cells, sponge bodies of nurse cells, and pre-oocyte in early stage egg chambers, and polar granules in the germ plasm at the posterior pole of mid-late stage oocytes and early embryos [13,14]. In these granules, Me31B interacts with other germ granule proteins and RNAs to exert post-transcriptional regulation on those RNAs [2,4,15]. For example, Me31B associates with germline-specific mRNA *oskar* (*osk;* encodes germ plasm inducer protein Osk) to prevent the premature translation of *osk* mRNA during its transport to the germ plasm [14,16–18].

Abbreviations
Aub, Aubergine; Bel, Belle; Bic-C, bicaudal-C; Dhc, dynein heavy chain; Eno, enolase; Khc, kinesin heavy chain; Klc, kinesin light chain; Pcm, Pacman; PfK, 6-phosphofructokinase; PgK, phosphoglycerate kinase; PyK, pyruvate kinase; RNPs, ribonucleoproteins; sDMA, symmetrically dimethylated arginine; Tral, trailer hitch; Tud, Tudor; Vas, Vasa.

Mapping the molecules that complex with Me31B and determining how they interact with Me31B is essential to understand the role and mechanism of Me31B in the germ granules. However, a Me31B interactome has not been completed. In this study, we used an *in vivo* crosslinking approach to isolate and identify the proteins in Me31B complexes. The obtained Me31B interactome contains polypeptides from four functional groups: RNA regulation proteins, glycolytic enzymes, cytoskeleton/motor proteins, and germ plasm proteins. We further showed that Me31B likely colocalizes with core germ plasm proteins Tudor (Tud), Vasa (Vas), and Aubergine (Aub) in both the nuage of nurse cells and the germ plasm of oocytes. We also provided evidence that Me31B could be a novel direct binding partner of Tud (a protein scaffold of germ plasm assembly). Our study revealed a dynamic interacting network of Me31B in *Drosophila* germ granules, supporting the role of Me31B in RNA post-transcriptional regulation and indicating its new functions in germ granule assembly and germline development.

Materials and methods

Drosophila strains

me31B-GFP and *vas* mutant strains were obtained from Bloomington Drosophila Stock Center as follows: *me31B-GFP* (stock # 51530), vas^1 (stock # 284), and *Df(2L)A72* (stock # 6058). *vas* mutant flies were generated by crossing vas^1 with *Df(2L)A72* flies. *tud* mutant flies were generated by crossing tud^1 with *Df(tud)* strains as previously described [19]. *HA-tud* flies in tud^1 background were generated as previously described [19]. *GFP* strain used as controls was previously described [13].

Drosophila ovary *in vivo* crosslinking

The ovary crosslinking method was adapted from the embryo *in vivo* crosslinking protocol previously described [20] with a few modifications. Particularly, freshly dissected Me31B-GFP or GPF ovaries were permeabilized by heptane on a rotary shaker for 5 min. The ovaries were then washed three times with PBST (PBS, 0.1% Triton X-100), each for 5 min. The washed ovaries were crosslinked with fixative solution (0.2% formaldehyde in PBST) for 10 min on a rotary shaker. After removing the fixative, quench solution (0.25 M glycine in PBST) was added to the ovaries and incubated on a rotary shaker for 5 min to stop the reaction. The ovaries were washed again with PBST three times, each for 5 min, and then used for immunoprecipitation or stored at −80 °C.

Isolation of crosslinked Me31B complexes

The purification of the crosslinked complex was performed essentially as described [20] with a few modifications. Crosslinked Me31B-GFP and GFP ovaries were homogenized in lysis buffer (PBS, 0.5 M Urea, 0.01% SDS, 2% Triton X-100, protease inhibitor) and immunoprecipitated with anti-GFP agarose beads (MBL). After washing the beads 10 times with high-stringency wash buffer (PBS, 0.1 M glycine, 1 M NaCl, 1% IGEPAL CA-630, and 0.1% Tween 20), the bound complexes were eluted from the beads with SDS-sample buffer at 65 °C for 10 min. The complexes were resolved on a 3–15% step gel (Fig. 1A) [20]. The formation of the complexes was visualized by

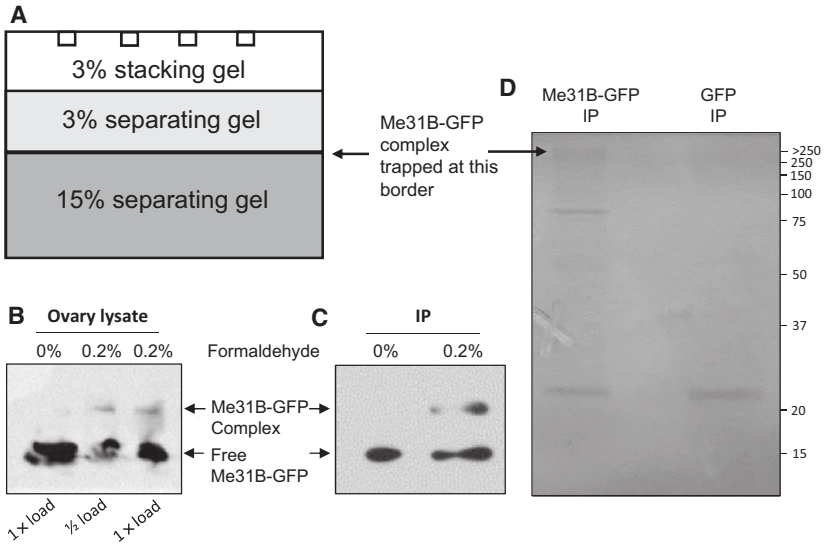

Fig. 1. Isolation of *in vivo* crosslinked Me31B complexes. (A) Illustration of the 3–15% step SDS/PAGE gel used to 'trap' the Me31B-GFP complexes. (B) 0.2% formaldehyde resulted in the formation of large molecular weight Me31B-GFP complexes in the ovary. (C) The Me31B-GFP complexes were also detected after lysate IP. (D) The Me31B-GFP complexes (indicated by arrow) were visualized on a Coomassie gel. Molecular weights of protein standards (kDa) are shown on the right.

anti-GFP western blot. For protein identification by mass spectrometry, the gel containing the complexes was stained with Coomassie blue (Thermo Fisher Scientific, Waltham, MA, USA), and then the gel band representing the Me31B-GFP complexes, as well as the gel band in the same position in the GFP control, were excised and analyzed.

Mass spectrometry identification of proteins

Purified proteins were denatured with 8 M urea and treated with 5 mM Tris (2-carboxyethyl) phosphine hydrochloride at 56 °C for 1 h to reduce disulfide bonds and then incubated with 5 mM iodoacetamide at 21 °C for 45 min to alkylate the reduced cysteine side chains and prevent formation of mixed disulfides. The solution was diluted to 1 M urea with 100 mM ammonium bicarbonate, and proteins were digested overnight with 1 μg trypsin. Tryptic peptides were analyzed using a Velos LTQ equipped with an Eksigent HPLC (replicate 1) or a Fusion Lumos mass spectrometer (replicates 2–4) equipped with an Easy-nLC 100 HPLC system (Thermo Scientific, Bremen, Germany). Peptides were separated using an acetonitrile-based gradient (Solvent A: 0% acetonitrile, 0.1% formic acid; Solvent B: 80% acetonitrile, 0.1% formic acid) at a flow rate of 300 $nL \cdot min^{-1}$. A 2-h gradient from 2% B to 40% B was used to elute the peptides. The resulting data were searched in Protein Prospector v5.19.4 (http://prospector.ucsf.edu) against the *D. melanogaster* Uniprot proteome, downloaded on 9/6/2016, which contained 42 452 sequences. A randomized 'decoy' database was concatenated to allow for estimation of global false discovery rates. Carbamidomethylation of cysteine residues was set as a fixed modification. Protein N-terminal acetylation, oxidation of methionine, protein N-terminal methionine loss, and pyroglutamine formation were set as variable modifications. A total of two variable modifications were allowed. Trypsin digestion specificity with one missed cleavage was allowed. The mass tolerance for precursor ions was set to 0.6 Da for the Velos data and 5 p.p.m. for the Orbitrap Fusion. Fragment ion tolerance was set to 0.6 Da for both instruments. Peptide and protein identification false discovery rates were set to 5%. Under these conditions, no proteins were found with two or more peptides in the decoy search.

Immunohistochemistry and imaging

Drosophila ovary immunostaining was performed as previously described [19,21]. Rabbit-anti-Me31B antibody was used at 1 : 2000 dilution. Rat-anti-Vas antibody was used at 1 : 500. Rat-anti-HA antibody (Roche Applied Science, Mannheim, Germany) was used at 1 : 350. Rat-anti-Aub antibody was used at 1 : 500. Goat-anti-rabbit-Alexa 488 secondary antibody and donkey-anti-rat-Cy3 secondary antibodies were both used at 1 : 500. Images of the stained egg chambers were captured by a laser scanning confocal microscope (Olympus IX71, Olympus Corporation, Center Valley, PA, USA).

Me31B-Tud direct binding assays

The binding assays were performed as previously described [22,23]. Briefly, equal amounts of Me31B-GFP and GFP proteins were immunoprecipitated from fly ovaries with anti-GFP agarose beads and remained bound to the beads. A representative gel image showing the purity of the Me31B-GFP protein IP is provided in Fig. S1. Purified HA-tagged Tud proteins were added in equal amounts to the Me31B-GFP beads and the GFP beads prepared above and incubated for 1 h with gentle agitation in binding buffer (PBS, 0.05% IGEPAL CA-630). The beads were washed three times with the binding buffer, and then the proteins were eluted from the beads with SDS-sample buffer. The eluted proteins were detected by using rat-anti-HA antibody (Roche, 1 : 2000) and rabbit-anti-GFP antibody (Abcam Cambridge, MA, USA; 1 : 10 000) in western blots. For the binding assay in the presence of RNase, 100 $\mu g \cdot mL^{-1}$ RNase A was added to the binding buffer during the 1-h binding, while PBS was added to the non-RNase controls instead. For binding assays in the presence of symmetrically dimethylated arginine (sDMA) peptides, HA-Tud proteins were preincubated with synthesized sDMA-containing peptides (MNLPPNPVIAR^{me2s}GR^{me2s}GR^{me2s}GR^{me2s}KPNNVEAN, 0.25 $mg \cdot mL^{-1}$; me2s denotes dimethylation) at 4 °C for 30 min, while control HA-Tud were preincubated with synthesized non-sDMA peptides (CPSSHSSLTERHKILHRLLQEGSPS).

Detection of symmetrically dimethylated arginine in Me31B

The detection of sDMA by SYM11 western blot was performed as previously described [22,24]. Particularly, GFP, Aub-GFP, and Me31B-GFP proteins were immunoprecipitated from 200 μL GFP ovaries, 200 μL Aub-GFP ovaries, and 50 μL Me31B-GFP ovaries, respectively, by using 20 μL anti-GFP beads (MBL, Woburn, MA, USA). In the western blots, SYM11 antibody (MilliporeSigma, St. Louis, MO, USA) was used at 1 : 500 followed by incubation with mouse anti-Rabbit-HRP secondary antibody (Jackson ImmunoResearch, West Grove, PA, USA; 1 : 2000). Rabbit-anti-GFP antibody (Abcam) was used at 1 : 100 000 with subsequent incubation with mouse-anti-Rabbit-HRP secondary antibody (Jackson ImmunoResearch, 1 : 20 000). The mass spectrometry detection of sDMAs was performed on Me31B-GFP proteins immunopurified from 200 μL Me31B-GFP ovaries.

Results and Discussion

In vivo crosslinking and immunoprecipitation effectively isolated Me31B complexes from *Drosophila* ovaries

Chemical crosslinking is a useful approach to capture transiently interacting molecules, especially in dynamic structures like germ granules [20,25]. Here, we adapted the previously reported embryo crosslinking protocol [20] to crosslink and isolate Me31B complexes from *Drosophila* ovarian tissue. In the ovaries, we used formaldehyde to crosslink GFP-tagged, endogenous Me31B proteins to their *in vivo* interacting molecules. To ensure specificity, we tested seven different concentrations of formaldehyde (from 0% to 4%), and we chose 0.2% for this study because it was the lowest concentration that allowed the formation of Me31B-GFP complexes. In the ovary lysate, we detected large molecular weight Me31B-GFP complexes 'trapped' at the 3–15% step gel border, separated from the noncrosslinked Me31B-GFP proteins (Fig. 1A,B). Then, we immunoprecipitated the complexes by using anti-GFP beads and observed the successful pull down of the complexes (Fig. 1C). We did note that a heterogeneous mixture of Me31B-containing complexes was isolated by using this method. Finally, we further gel-purified the complexes and, on a Coomassie-stained gel, obtained a visible protein band that corresponded to the Me31B-GFP complexes (Fig. 1D), which was excised for protein identification analysis by mass spectrometry. As a control, we performed the above procedure with fly ovaries expressing GFP alone and did not detect the formation of complexes containing GFP (Fig. 1D). This underscores the specificity of our crosslinking. Nevertheless, the 'empty' gel band in the GFP control that corresponded to the protein band of the Me31B-GFP complexes was analyzed in parallel, and the proteins found were used to control for false positive results.

Me31B interacts with germ granule proteins from four functional groups

In multiple independently isolated Me31B complexes, we consistently identified the proteins listed in Table 1. According to the known functions of the proteins, they fall into four groups: RNA regulation factors, glycolytic enzymes, cytoskeleton/motor proteins, and germ plasm proteins.

RNA regulation proteins (translation repressors)

Cup, trailer hitch (Tral), Belle (Bel), and Bic-C proteins are often involved in the translational repression of germline mRNAs and are known to complex with Me31B. Cup protein modulates target RNAs by a combined mechanism of translational repression and promoting deadenylation [26–28]. For example, Cup forms a complex with Me31B and Tral on *osk* mRNA (encoding germ plasm inducer protein Osk) and represses its translation during early oogenesis. Interestingly, the Cup-Me31B interaction in the *osk* repression complex was RNase sensitive, indicating that Cup–Me31B interaction is RNA dependent [26]. However, the loss of Cup does not obviously change the protein level or the localization pattern of Me31B [29], suggesting that Cup and Me31B may bind independently to the same RNA but cooperatively repress its translation. Tral directly binds Me31B through its

Table 1. Proteins identified in the Me31B complexes using *in vivo* crosslinking.

Proteins	Granule type	Me31B/ GFP ratio[a]
RNA regulation proteins		
Cup	P body, nuage, germ plasm	4.20
Tral	P body, nuage, germ plasm	4.36
Bel	Nuage, germ plasm	High
Bic-C	P body	High
Edc3	P body	7.00
Pcm	P body	High
NOT1	P body	75.00
eIF4G		19.60
eIF4E		5.00
Cytoskeleton and motor proteins		
Dhc 64C	Germ plasm	84.50
Khc		50.00
Klc		High
β-Tubulin (BetaTub56D)		7.29
Glycolytic enzymes		
PyK	Germ plasm	41.00
PgK	Germ plasm	High
Eno		High
PfK		High
Germ plasm proteins		
Tud	Nuage, germ plasm	31.50
Vas	Nuage, germ plasm	19.00
Aub	Nuage, germ plasm	High
eIF4A	Germ plasm	High

[a] The enrichment ratio for each protein was calculated by dividing the average number of peptides in the Me31B IP by the average number of peptides in the GFP control. In those cases where we never found a protein in the GFP control, the enrichment ratio was labeled as 'high'. The number of peptides identified (for each protein) in each of the four biological replicates as well as the total number identified in the corresponding GFP control are provided in Table S1.

conserved FDF domain and is usually found in the same germ granules with Me31B [30,31]. As an example, the Tral–Me31B complex may exist in multiple copies and coat along the length of *nanos* (*nos*) mRNA to repress its translation [32]. In addition, the Tral–Me31B complex also interacts with piRNA pathway (a small RNA-guided antitransposon system) proteins, PAPI and Ago3, in the nuage, suggesting a physical and functional link between the Tral–Me31B complex and piRNA-mediated mRNA regulation [30]. Bel, similar to Me31B, is a DEAD-box ATP-dependent RNA helicase required for viability and germline development [33]. It complexes with Me31B and Tral on *nos* mRNA and is involved in the deadenylation and repression of the mRNA [32]. Bicaudal-C (Bic-C) is an RNA-binding protein that associates with many ovarian RNAs to regulate their expression [34]. For example, Bic-C is required for the proper localization and translational repression of *osk* mRNA during oogenesis [35,36]. It also associates with Tral–Me31B complex for the proper localization of *gurken* (*grk*) mRNA and Grk protein [37]. These studies suggest that Bic-C complexes with Me31B and works simultaneously in the translational repression of germline RNAs.

RNA regulation proteins (RNA degraders)

Enhancer of decapping-3 (EDC3), Pacman (Pcm; XRN1), and NOT1 are common P body components involved in general cytoplasmic mRNA degradation. EDC3 associates with Dcp1 and Dcp2 decapping proteins to stimulate the activity of the Dcp1–Dcp2 complex [38,39]. Like Tral, EDC3 also interacts with Me31B through the FDF motifs, and this interaction is required to repress the translation of target mRNA *in vitro* [31]. Pacman (XRN1) is a cytoplasmic 5′→3′ exoribonuclease needed for egg chamber development and egg production [40]. In P bodies, it directly interacts with Dcp1 and is responsible for degrading the mRNAs after decapping [41,42]. NOT1 is the scaffold of the CCR4–NOT complex, which catalyzes mRNA deadenylation in *Drosophila* ovaries [43]. This indicates the recruitment of the CCR4–NOT deadenylation complex into the Me31B RNP. Indeed, Bic-C and Cup in Me31B complexes can recruit the deadenylation complex to target mRNAs [28,34]. Interestingly, NOT1 associates with RNA-binding protein Ataxin-2 (ATX2) in a Me31B-dependent manner in *Drosophila* circadian pacemaker neurons, where the NOT1–Me31B—ATX2 complex plays a role in post-transcriptional gene silencing [44]. The existence or function of such a complex in germ cells remains unclear.

Translation initiation factors eIF4E and eIF4G were uncovered in the Me31B complexes, indicating a Cup-eIF4E-mediated repression mechanism for the mRNAs in the Me31B complexes. The interaction between the cap-binding protein eIF4E and scaffold-like protein eIF4G is critical for successful mRNA translation. Cup, an eIF4E-binding protein, competes with eIF4G for eIF4E binding, disrupts the assembly of translation initiation complex, and, therefore, inhibits translation [26,28].

Cytoskeleton and motor proteins

Microtubule cytoskeleton protein beta-tubulin and three motor proteins, dynein heavy chain (Dhc), kinesin heavy chain (Khc), and kinesin light chain (Klc), were found in the Me31B complexes, indicating the microtubule-motor protein-dependent transportation mechanism for the Me31B complexes. Indeed, *osk* mRNA forms a complex with Me31B, and its transportation and localization relies on microtubules [7,14,45]. Dynein and kinesin motors are required for the motility, anchoring, and distribution of germ plasm components during oogenesis [46], and dynein-dependent transport ensures their segregation into forming germ cells [45]. Furthermore, Dhc was shown to colocalize with Vas in the germ plasm, and, together with Khc, was found to complex with core germ plasm proteins Aub and Tud [23], consistent with our model that Me31B interacts with Aub and Tud (see below and Fig. 2).

Glycolytic enzymes

Four glycolytic enzymes, pyruvate kinase (PyK), enolase (Eno), 6-phosphofructokinase (PfK), and phosphoglycerate kinase (PgK), were identified in the Me31B complexes. In accordance with our data, PyK and PgK were found in polar granules by immuno-EM [22]. Furthermore, PyK and Eno are both found in Tud and Aub complexes [23], and PyK directly binds to Tud and contains sDMA [22]. Considering that Me31B may bind to Tud in a similar way (see below), we propose a model where the glycolytic enzymes are linked to Me31B via scaffold protein Tud (Fig. 2). The glycolytic enzymes in Me31B complexes may provide ATP to support the functioning of ATP-dependent helicases like Me31B, Bel, eIF4A, and Vas in the remodeling of germ granule RNPs. Aside from the well-characterized functions of glycolytic enzymes in energy metabolism, recent studies on the RNA-binding proteome of yeast, nematode, and cultured human cells showed that these enzymes are conserved

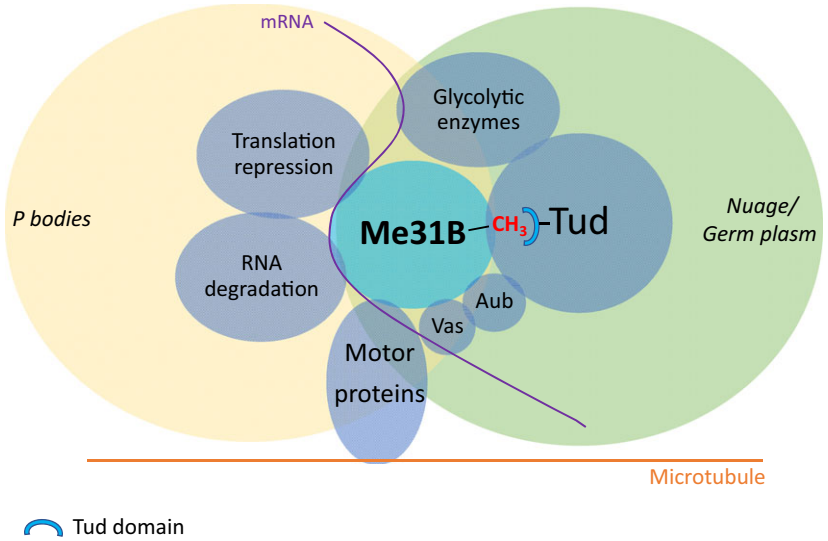

Fig. 2. Model of Me31B interactome in *Drosophila* germline RNP granules. In this model, Me31B exists in different types of granules, P bodies and germ granules (nuage, and polar granules in germ plasm). In P body granules, Me31B interacts with translational repressor proteins and RNA degrader proteins to repress the translation of the target mRNAs and degrade them, rendering post-transcriptional regulation of the mRNAs. In germ granules, Me31B interacts with core nuage/germ plasm proteins Tud, Vas, and Aub. Particularly, Me31B may directly binds to the Tud domains of Tud protein using sDMA. Glycolytic enzymes in the Me31B complexes may provide glycolytic ATP for the ATP-dependent RNA helicases or directly bind RNAs therein for the regulation and remodeling of germ granule RNPs, and for the motor proteins to transport the RNPs along microtubule cytoskeleton.

RNA-binding proteins [47–49]. Glycolytic enzymes are therefore speculated to 'moonlight' as post-transcriptional regulators. Together with the finding of four glycolytic enzymes in the Me31B RNP, we speculate that these enzymes may also play noncanonical roles like binding to and regulating certain germ granule RNAs.

Germ plasm proteins

Surprisingly, we found three core germ plasm proteins in the Me31B complexes: Tud, Vas, and Aub, which are essential for the assembly and functions of germ granules in the nuage and germ plasm (for review see refs [1,3,8]). Tud is a large protein with 11 protein-binding domains, Tud domains, which bind to sDMAs of other proteins like Aub. In this way, Tud functions as a scaffold that recruits other proteins during germ plasm assembly [22,24,50]. Vas is a DEAD-box RNA helicase that plays essential roles in the piRNA pathway in the nuage and interacts with Osk to initiate germ plasm assembly in mid-stage oocytes [51–53]. Aub is a critical nuclease component of the piRNA pathway, in which Aub produces piRNAs and uses them as a guide to silence transposons or degrade certain maternal mRNAs [54–56]. Finding these three core germ plasm proteins in the Me31B complexes suggests that they may interact with Me31B in germ granules.

Me31B shows similar localization pattern with germ granule proteins Tud, Vas, and Aub in the nuage and germ plasm

We continued by asking whether Me31B indeed interacts with Tud, Vas, and Aub. Previous *in vitro* crosslinking studies showed that Me31B is present in Vas and Tud complexes isolated from early *Drosophila* embryos [13]; however, whether they interact in different ovarian germ granules *in vivo* is not clear. To this end, we performed immunostaining in *Drosophila* egg chambers to examine whether Me31B has the same localization pattern as these germ plasm proteins. Since available anti-Me31B and anti-Tud antibodies are generated in the same species, we used *HA-tud* transgene expressed in *tud* protein null (tud^1) background to study Me31B-Tud localization pattern. The *HA-tud* transgenic flies showed no defect in any aspect of development compared to the wild-type [19], and Me31B's localization pattern in *HA-tud* flies was indistinguishable to that of the wild-type flies (data not shown), justifying the use of *HA-tud* flies as the wild-type control. We found that Me31B and HA-Tud showed similar localization pattern in both the nuage of nurse cells and the germ plasm of oocytes (Fig. 3A). Me31B showed a particulate staining in the nuage. We note that there are some Me31B particles that do not seem to overlap with HA-Tud in the perinuclear region, and our data indicate partial

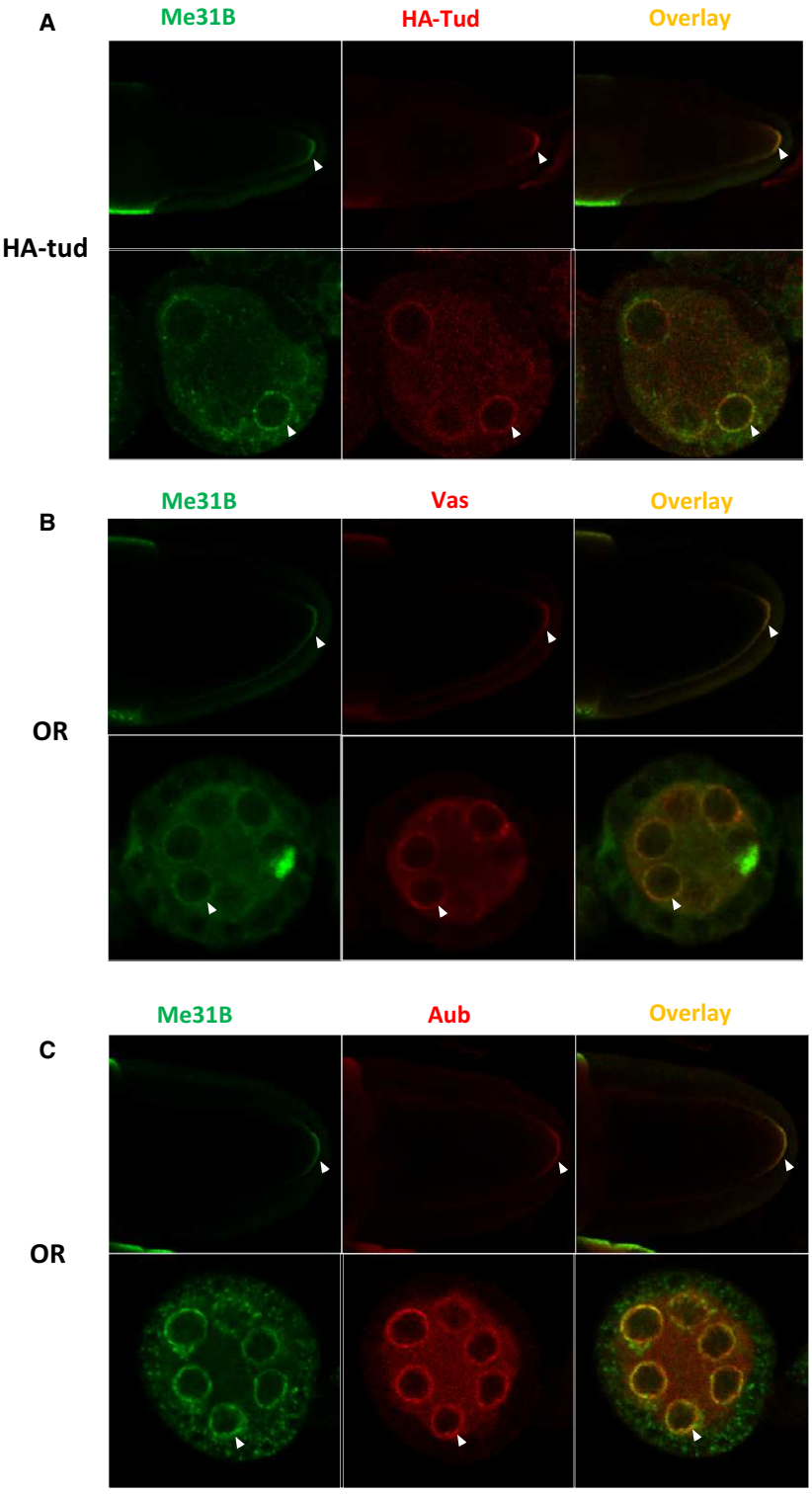

Fig. 3. Me31B shows similar localization pattern with germ plasm proteins Tud, Vas, and Aub. (A) Me31B (green channel) showed similar localization pattern with HA-Tud (red channel) in the germ plasm of oocyte (top panels) and in the nuage of nurse cells (bottom panels) in *HA-tud* transgenic flies. (B) Me31B (green channel) showed the similar localization pattern with Vas (red channel) in the germ plasm (top panels) and in the nuage (bottom panels) in wild-type Oregon-R (OR) flies. (C) Me31B (green channel) showed similar localization pattern with Aub (red channel) in the germ plasm (top panels) and in the nuage (bottom panels) in OR flies. The posterior of the oocytes at the top panels is to the right. Germ plasm and nuage are indicated with arrowheads.

overlapping between the two proteins in the nuage (Fig. 3A). Furthermore, we observed similar localization for Me31B-Vas and Me31B-Aub (Fig. 3B,C), with Me31B-Aub showing the most obvious overlapping in the nuage. Together with our crosslinking data, we conclude that Me31B may interact with Tud, Vas, and Aub in both the nuage and the oocyte's polar granules and that the colocalization between Me31B and the three

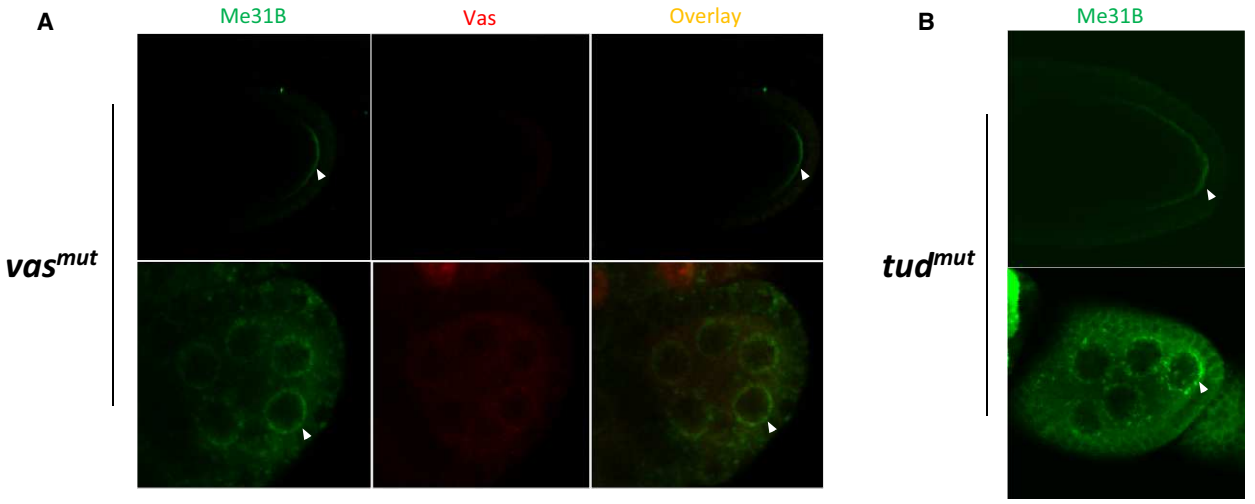

Fig. 4. Me31B localizes to germ plasm and nuage in *vas* and *tud* mutants. (A) Me31B (green channel) localizes to germ plasm (top panels) and nuage (bottom panels) in *vas* mutant ovaries. Vas, red channel. (B) Me31B (green channel) localizes to germ plasm (top panel) and nuage (bottom panel) in *tud* mutant ovaries. The posterior of the oocytes at the top panels is to the right. Germ plasm and nuage are indicated with arrowheads.

germ plasm proteins in those locations is likely. Our ovarian staining results are consistent with previous EM work on *Drosophila* embryos which showed the localization of Me31B, Tud, Vas, and Aub to embryonic polar granules [13,57]. Considering that Tud, Vas, and Aub occupy the same space within a germ plasm granule [8], we speculate that a Me31B–Tud–Vas–Aub complex may exist in the nuage and the germ plasm. However, the assembly of this complex in the two locations is most likely independent since nuage particles are not the precursors of germ plasm granules [58].

Me31B localization to the nuage and germ plasm is independent of Vas and Tud

Next, we asked how Me31B is recruited to the Tud-Vas-Aub germ plasm/nuage complexes. The fact that Vas and Tud are both involved in the stepwise assembly of germ plasm [19,59] raises the possibility that Me31B's localization to these granules may depend on Vas or Tud. To investigate this, we performed Me31B immunostaining in *vas* and *tud* mutant ovaries. Surprisingly, Me31B's localization to the nuage and germ plasm in both mutants was comparable to that in the wild-type (Fig. 4A,B). Using germline clone or RNAi techniques, mutation in or knockdown of *me31B* caused severe egg chamber degeneration in early- to mid-oogenesis ([14] and our unpublished data). Therefore, the possibility that Me31B acts upstream of Vas and Tud in germ granule assembly was not tested. We conclude that Me31B's localization to the nuage and germ plasm does not depend on Vas or Tud; instead, Me31B may act upstream of or in parallel with Vas and Tud in the assembly pathway.

Me31B binds to Tud in an sDMA-dependent manner

Next, we sought a biochemical approach to study the interaction mechanism between Me31B and Tud. In this study, we focused on Tud, since it is a scaffold molecule containing Tud domains that bind to the sDMAs of proteins like Aub to recruit them to the germ plasm [19,21]. To find out if Me31B–Tud interaction occurs in this manner, we performed *in vitro* binding assays. HA-Tud proteins expressed and purified from Sf9-baculovirus system were added to Me31B-GFP, GFP, and Aub-GFP-bound beads. We observed the binding of HA-Tud with Me31B-GFP and Aub-GFP-bound beads but not with GFP beads (Fig. 5A), suggesting a protein–protein interaction between Me31B and Tud.

Since Me31B has potential RNA-binding activity, it is possible that Me31B-Tud binding is mediated by RNA. To test this possibility, we performed the binding assay in the presence of RNase. The results showed that RNase treatment did not inhibit the Me31B-Tud binding, indicating that the Me31B-Tud binding is RNA independent (Fig. 5B). We note that the RNase treatment caused a decrease in HA-Tud binding, to a very similar extent, to all the tested proteins including the positive control Aub, which is a known direct binding partner of Tud. Therefore, we

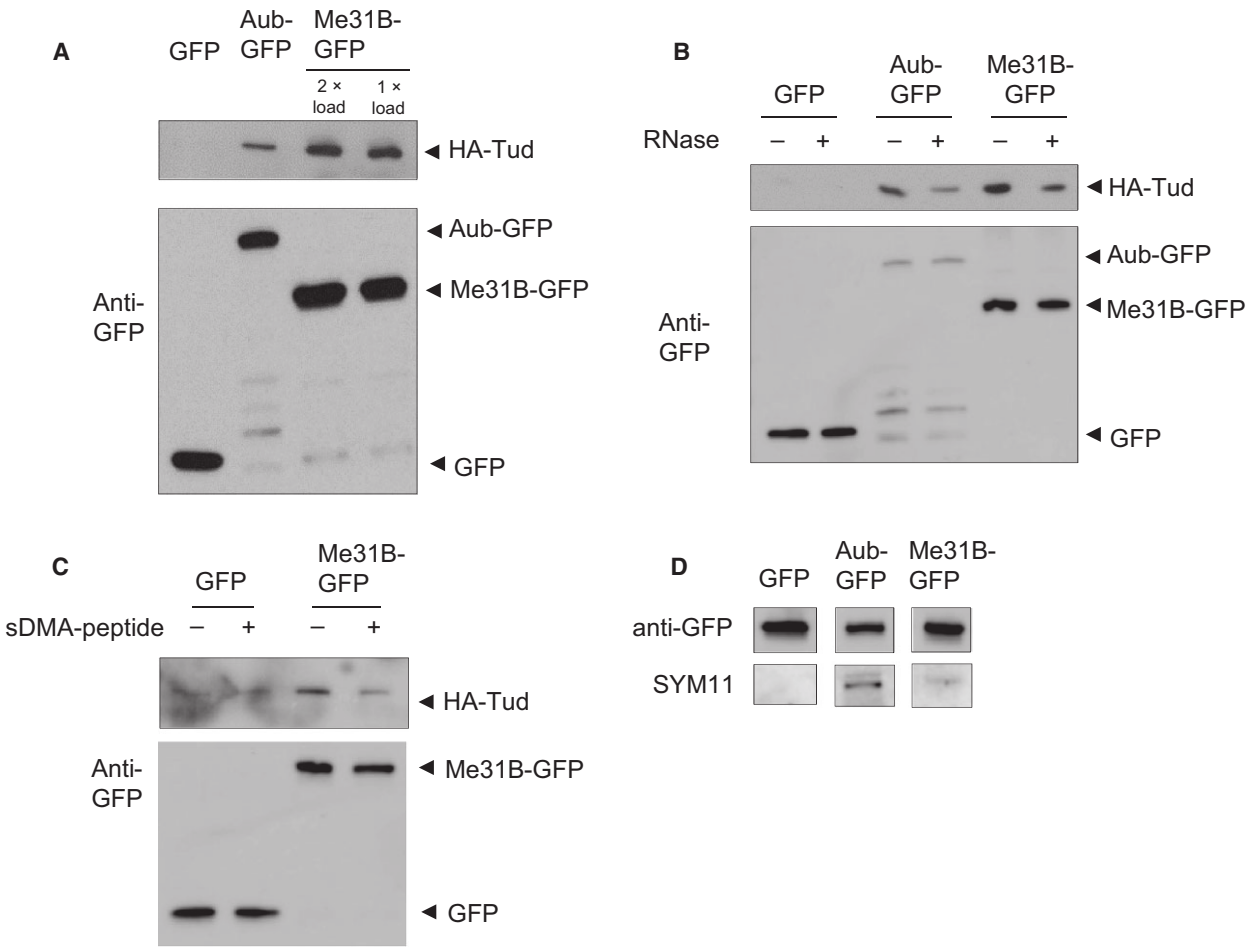

Fig. 5. Me31B binds to Tud in an *in vitro* binding assay. (A) Me31B-GFP bound beads showed binding to HA-Tud protein (right lanes). Positive control Aub-GFP also showed binding to HA-Tud (middle lane). Negative control GFP showed no binding to HA-Tud (left lane). (B) Me31B-GFP still showed binding to HA-Tud in the presence of RNase (right lanes). Positive control Aub-GFP also showed binding to HA-Tud in the presence of RNase as expected (middle lanes), but negative control GFP showed no binding or negligible binding with or without RNase, respectively (left lanes). (C) sDMA peptide caused reduced binding of Me31B-GFP to HA-Tud (last lane) when comparing to non-sDMA peptide control. GFP control showed no binding to HA-Tud with or without the peptide (left lanes). (D) Me31B-GFP showed positive signal in SYM11 western blot (last lane). Positive control Aub-GFP produced strong signal (middle lane) and GFP did not produce any signal (left lane). The uncropped image of Fig. 5D is provided in Fig. S2.

reason that the addition of RNase may have caused a universal decrease in HA-Tud binding under our experimental conditions.

Next, we asked if Me31B-Tud binding occurs via the known sDMA–Tud domain recognition mechanism. We performed a competitive-binding assay using sDMA-containing peptides. These synthesized peptides originate from the N-terminal sequence of Aub and contain multiple sDMAs (see Materials and methods). When bound by an excessive amount of the peptides, Tud loses binding to other sDMA-containing proteins [22]. The results showed that, compared to the non-treated HA-Tud, the sDMA peptide-quenched HA-Tud bound significantly less on the Me31B-GFP beads. This indicates that Me31B–Tud interaction depends on sDMA-Tud domain recognition (Fig. 5C).

The next apparent question was whether Me31B contains sDMAs. To answer this, we performed a western blot on Me31B proteins using SYM11 antibody that was successfully used for the identification of sDMAs in Aub, Vas, and PyK [22,24,60]. Using Me31B-GFP proteins purified from fly ovaries, we detected positive SYM11 signal from Me31B-GFP (Fig. 5D). Interestingly, we noticed that Me31B's SYM11 signal was much weaker than that of the positive control Aub-GFP protein (Fig. 5D). Since Aub contains several sDMAs [24], we reasoned that the SYM11 signal strength may reflect the quantity of the sDMAs in a protein. Indeed, using

purified Me31B and direct mass spectrometry analysis, we detected the presence of a single sDMA residue in Me31B. The importance of this sDMA for Tud binding and the assembly of germ granules will be a subject of future investigation. Taken together, our data strongly suggest that Me31B could be a novel direct binding partner of Tud and that the binding occurs in an sDMA-Tud domain-dependent manner.

Model of Me31B interactome in *Drosophila* germ granules

In this study, we used a proteomics approach to map the *in vivo* interactome of an important *Drosophila* germ granule protein, Me31B. The effectiveness of this method allows general application to the interactome study of other ovarian proteins. Using this method, we found that Me31B interacts with proteins from four functional groups: RNA regulation proteins (translational repressors and RNA degraders), glycolytic enzymes, cytoskeleton/motor proteins, and germ plasm proteins. We further showed that Me31B may interact with core germ plasm proteins Tud, Vas, and Aub in the nuage and germ plasm and provided biochemical evidence showing that Me31B may directly bind to Tud domains of scaffold protein Tud. We summarize by proposing a Me31B interactome model (Fig. 2) where Me31B takes part in three different types of RNP granules: P bodies, nuage, and polar granules in germ plasm. In P bodies, Me31B complexes with RNA regulation proteins to confer post-transcriptional control over the mRNAs via translational repression and RNA degradation. Glycolytic enzymes in the complexes may directly bind RNAs and generate local ATP to support the functioning of RNA helicases and motor proteins in RNA translational regulation, RNA transportation, and germ granule (nuage and germ plasm's polar granules) remodeling. Cytoskeleton/motor proteins provide a means for the transportation of the Me31B complexes. In the nuage and germ plasm, Me31B interacts with Tud, Vas, and Aub, suggesting Me31B's possible new roles in germ granule assembly and function. These Me31B-containing granules may physically interact and dynamically exchange components [4,11,61]. However, whether Me31B plays the same, partially overlapping, or distinct roles in these different granules awaits further research.

Acknowledgements

We thank Peter Avis and Xue Wang for revising the manuscript. This work was supported by Indiana University Northwest Start-Up Fund and Faculty Summer Fellowship to MG and by National Science Foundation grant awards CAREER MCB-1054962 and MCB-1715541 to ALA. We thank Akira Nakamura for anti-Me31B antibody and Paul Lasko for anti-Vas and anti-Aub antibodies. Also, we thank Bloomington Drosophila Stock Center for providing fly lines.

Author contributions

MG conceived and supervised the study; HD, AM, CC, BA, DS, and MG designed and performed the experiments; JCT carried out mass spectrometry identification of proteins; ALA and MG wrote the manuscript.

References

1 Gao M and Arkov AL (2013) Next generation organelles: structure and role of germ granules in the germline. *Mol Reprod Dev* **80**, 610–623.
2 Arkov AL and Ramos A (2010) Building RNA-protein granules: insight from the germline. *Trends Cell Biol* **20**, 482–490.
3 Lehmann R (2016) Germ plasm biogenesis – an oskar-centric perspective. *Curr Top Dev Biol* **116**, 679–707.
4 Voronina E, Seydoux G, Sassone-Corsi P and Nagamori I (2011) RNA granules in germ cells. *Cold Spring Harb Perspect Biol* **3**, a002774.
5 Swartz SZ and Wessel GM (2015) Germ line versus soma in the transition from egg to embryo. *Curr Top Dev Biol* **113**, 149–190.
6 Strome S and Updike D (2015) Specifying and protecting germ cell fate. *Nat Rev Mol Cell Biol* **16**, 406–416.
7 Becalska AN and Gavis ER (2009) Lighting up mRNA localization in *Drosophila* oogenesis. *Development* **136**, 2493–2503.
8 Trcek T, Grosch M, York A, Shroff H, Lionnet T and Lehmann R (2015) *Drosophila* germ granules are structured and contain homotypic mRNA clusters. *Nat Commun* **6**, 7962.
9 Kloc M, Bilinski S and Etkin LD (2004) The Balbiani body and germ cell determinants: 150 years later. *Curr Top Dev Biol* **59**, 1–36.
10 Kloc M, Jedrzejowska I, Tworzydlo W and Bilinski SM (2014) Balbiani body, nuage and sponge bodies–term plasm pathway players. *Arthropod Struct Dev* **43**, 341–348.
11 Gallo CM, Munro E, Rasoloson D, Merritt C and Seydoux G (2008) Processing bodies and germ granules are distinct RNA granules that interact in *C. elegans* embryos. *Dev Biol* **323**, 76–87.
12 Weston A and Sommerville J (2006) Xp54 and related (DDX6-like) RNA helicases: roles in messenger RNP assembly, translation regulation and RNA degradation. *Nucleic Acids Res* **34**, 3082–3094.

13 Thomson T, Liu N, Arkov A, Lehmann R and Lasko P (2008) Isolation of new polar granule components in *Drosophila* reveals P body and ER associated proteins. *Mech Dev* **125**, 865–873.
14 Nakamura A, Amikura R, Hanyu K and Kobayashi S (2001) Me31B silences translation of oocyte-localizing RNAs through the formation of cytoplasmic RNP complex during *Drosophila* oogenesis. *Development* **128**, 3233–3242.
15 Rangan P, DeGennaro M, Jaime-Bustamante K, Coux RX, Martinho RG and Lehmann R (2009) Temporal and spatial control of germ-plasm RNAs. *Curr Biol* **19**, 72–77.
16 Ephrussi A, Dickinson LK and Lehmann R (1991) Oskar organizes the germ plasm and directs localization of the posterior determinant nanos. *Cell* **66**, 37–50.
17 Kim-Ha J, Kerr K and Macdonald PM (1995) Translational regulation of oskar mRNA by bruno, an ovarian RNA-binding protein, is essential. *Cell* **81**, 403–412.
18 Markussen FH, Michon AM, Breitwieser W and Ephrussi A (1995) Translational control of oskar generates short OSK, the isoform that induces pole plasma assembly. *Development* **121**, 3723–3732.
19 Arkov AL, Wang JY, Ramos A and Lehmann R (2006) The role of Tudor domains in germline development and polar granule architecture. *Development* **133**, 4053–4062.
20 Gao M, McCluskey P, Loganathan SN and Arkov AL (2014) An in vivo crosslinking approach to isolate protein complexes from *Drosophila* embryos. *J Vis Exp* **86**, e51387.
21 Creed TM, Loganathan SN, Varonin D, Jackson CA and Arkov AL (2010) Novel role of specific Tudor domains in Tudor-Aubergine protein complex assembly and distribution during *Drosophila* oogenesis. *Biochem Biophys Res Commun* **402**, 384–389.
22 Gao M, Thomson TC, Creed TM, Tu S, Loganathan SN, Jackson CA, McCluskey P, Lin Y, Collier SE, Weng Z *et al.* (2015) Glycolytic enzymes localize to ribonucleoprotein granules in *Drosophila* germ cells, bind Tudor and protect from transposable elements. *EMBO Rep* **16**, 379–386.
23 Zheng J, Gao M, Huynh N, Tindell SJ, Vo HD, McDonald WH and Arkov AL (2016) In vivo mapping of a dynamic ribonucleoprotein granule interactome in early *Drosophila* embryos. *FEBS Open Bio* **6**, 1248–1256.
24 Kirino Y, Vourekas A, Sayed N, de Lima Alves F, Thomson T, Lasko P, Rappsilber J, Jongens TA and Mourelatos Z (2010) Arginine methylation of Aubergine mediates Tudor binding and germ plasm localization. *RNA* **16**, 70–78.
25 Vourekas A and Mourelatos Z (2014) HITS-CLIP (CLIP-Seq) for mouse Piwi proteins. *Methods Mol Biol* **1093**, 73–95.
26 Nakamura A, Sato K and Hanyu-Nakamura K (2004) *Drosophila* cup is an eIF4E binding protein that associates with Bruno and regulates oskar mRNA translation in oogenesis. *Dev Cell* **6**, 69–78.
27 Wilhelm JE, Hilton M, Amos Q and Henzel WJ (2003) Cup is an eIF4E binding protein required for both the translational repression of oskar and the recruitment of Barentsz. *J Cell Biol* **163**, 1197–1204.
28 Igreja C and Izaurralde E (2011) CUP promotes deadenylation and inhibits decapping of mRNA targets. *Genes Dev* **25**, 1955–1967.
29 Broyer RM, Monfort E and Wilhelm JE (2017) Cup regulates oskar mRNA stability during oogenesis. *Dev Biol* **421**, 77–85.
30 Liu L, Qi H, Wang J and Lin H (2011) PAPI, a novel TUDOR-domain protein, complexes with AGO3, ME31B and TRAL in the nuage to silence transposition. *Development* **138**, 1863–1873.
31 Tritschler F, Braun JE, Eulalio A, Truffault V, Izaurralde E and Weichenrieder O (2009) Structural basis for the mutually exclusive anchoring of P body components EDC3 and Tral to the DEAD box protein DDX6/Me31B. *Mol Cell* **33**, 661–668.
32 Gotze M, Dufourt J, Ihling C, Rammelt C, Pierson S, Sambrani N, Temme C, Sinz A, Simonelig M and Wahle E (2017) Translational repression of the *Drosophila* nanos mRNA involves the RNA helicase Belle and RNA coating by Me31B and Trailer hitch. *RNA* **10**, 1552–1568.
33 Johnstone O, Deuring R, Bock R, Linder P, Fuller MT and Lasko P (2005) Belle is a *Drosophila* DEAD-box protein required for viability and in the germ line. *Dev Biol* **277**, 92–101.
34 Chicoine J, Benoit P, Gamberi C, Paliouras M, Simonelig M and Lasko P (2007) Bicaudal-C recruits CCR4-NOT deadenylase to target mRNAs and regulates oogenesis, cytoskeletal organization, and its own expression. *Dev Cell* **13**, 691–704.
35 Mahone M, Saffman EE and Lasko PF (1995) Localized bicaudal-C RNA encodes a protein containing a KH domain, the RNA binding motif of FMR1. *EMBO J* **14**, 2043–2055.
36 Saffman EE, Styhler S, Rother K, Li W, Richard S and Lasko P (1998) Premature translation of oskar in oocytes lacking the RNA-binding protein bicaudal-C. *Mol Cell Biol* **18**, 4855–4862.
37 Kugler JM, Chicoine J and Lasko P (2009) Bicaudal-C associates with a Trailer Hitch/Me31B complex and is required for efficient Gurken secretion. *Dev Biol* **328**, 160–172.
38 Tritschler F, Eulalio A, Truffault V, Hartmann MD, Helms S, Schmidt S, Coles M, Izaurralde E and Weichenrieder O (2007) A divergent Sm fold in EDC3 proteins mediates DCP1 binding and P-body targeting. *Mol Cell Biol* **27**, 8600–8611.

39 Fromm SA, Truffault V, Kamenz J, Braun JE, Hoffmann NA, Izaurralde E and Sprangers R (2012) The structural basis of Edc3- and Scd6-mediated activation of the Dcp1:Dcp2 mRNA decapping complex. *EMBO J* **31**, 279–290.
40 Lin MD, Jiao X, Grima D, Newbury SF, Kiledjian M and Chou TB (2008) *Drosophila* processing bodies in oogenesis. *Dev Biol* **322**, 276–288.
41 Nagarajan VK, Jones CI, Newbury SF and Green PJ (2013) XRN 5'–>3' exoribonucleases: structure, mechanisms and functions. *Biochim Biophys Acta* **1829**, 590–603.
42 Braun JE, Truffault V, Boland A, Huntzinger E, Chang CT, Haas G, Weichenrieder O, Coles M and Izaurralde E (2012) A direct interaction between DCP1 and XRN1 couples mRNA decapping to 5' exonucleolytic degradation. *Nat Struct Mol Biol* **19**, 1324–1331.
43 Temme C, Simonelig M and Wahle E (2014) Deadenylation of mRNA by the CCR4-NOT complex in *Drosophila*: molecular and developmental aspects. *Front Genet* **5**, 143.
44 Lee J, Yoo E, Lee H, Park K, Hur JH and Lim C (2017) LSM12 and ME31B/DDX6 define distinct modes of posttranscriptional regulation by ATAXIN-2 protein complex in *Drosophila* circadian pacemaker neurons. *Mol Cell* **66**, 129–140 e7.
45 Lerit DA and Gavis ER (2011) Transport of germ plasm on astral microtubules directs germ cell development in *Drosophila*. *Curr Biol* **21**, 439–448.
46 Sinsimer KS, Lee JJ, Thiberge SY and Gavis ER (2013) Germ plasm anchoring is a dynamic state that requires persistent trafficking. *Cell Rep* **5**, 1169–1177.
47 Beckmann BM, Horos R, Fischer B, Castello A, Eichelbaum K, Alleaume AM, Schwarzl T, Curk T, Foehr S, Huber W *et al.* (2015) The RNA-binding proteomes from yeast to man harbour conserved enigmRBPs. *Nat Commun* **6**, 10127.
48 Castello A, Fischer B, Eichelbaum K, Horos R, Beckmann BM, Strein C, Davey NE, Humphreys DT, Preiss T, Steinmetz LM *et al.* (2012) Insights into RNA biology from an atlas of mammalian mRNA-binding proteins. *Cell* **149**, 1393–1406.
49 Matia-Gonzalez AM, Laing EE and Gerber AP (2015) Conserved mRNA-binding proteomes in eukaryotic organisms. *Nat Struct Mol Biol* **22**, 1027–1033.
50 Liu H, Wang JY, Huang Y, Li Z, Gong W, Lehmann R and Xu RM (2010) Structural basis for methylarginine-dependent recognition of Aubergine by Tudor. *Genes Dev* **24**, 1876–1881.
51 Xiol J, Spinelli P, Laussmann MA, Homolka D, Yang Z, Cora E, Coute Y, Conn S, Kadlec J, Sachidanandam R *et al.* (2014) RNA clamping by Vasa assembles a piRNA amplifier complex on transposon transcripts. *Cell* **157**, 1698–1711.
52 Jeske M, Muller CW and Ephrussi A (2017) The LOTUS domain is a conserved DEAD-box RNA helicase regulator essential for the recruitment of Vasa to the germ plasm and nuage. *Genes Dev* **31**, 939–952.
53 Dehghani M and Lasko P (2016) C-terminal residues specific to Vasa among DEAD-box helicases are required for its functions in piRNA biogenesis and embryonic patterning. *Dev Genes Evol* **226**, 401–412.
54 Wang W, Han BW, Tipping C, Ge DT, Zhang Z, Weng Z and Zamore PD (2015) Slicing and binding by Ago3 or Aub trigger Piwi-bound piRNA production by distinct mechanisms. *Mol Cell* **59**, 819–830.
55 Han BW, Wang W, Li C, Weng Z and Zamore PD (2015) Noncoding RNA. piRNA-guided transposon cleavage initiates Zucchini-dependent, phased piRNA production. *Science* **348**, 817–821.
56 Barckmann B, Pierson S, Dufourt J, Papin C, Armenise C, Port F, Grentzinger T, Chambeyron S, Baronian G, Desvignes JP *et al.* (2015) Aubergine iCLIP reveals piRNA-dependent decay of mRNAs involved in germ cell development in the early embryo. *Cell Rep* **12**, 1205–1216.
57 Bardsley A, McDonald K and Boswell RE (1993) Distribution of tudor protein in the *Drosophila* embryo suggests separation of functions based on site of localization. *Development* **119**, 207–219.
58 Snee MJ and Macdonald PM (2004) Live imaging of nuage and polar granules: evidence against a precursor-product relationship and a novel role for Oskar in stabilization of polar granule components. *J Cell Sci* **117**, 2109–2120.
59 Lasko P (2013) The DEAD-box helicase Vasa: evidence for a multiplicity of functions in RNA processes and developmental biology. *Biochim Biophys Acta* **1829**, 810–816.
60 Kirino Y, Vourekas A, Kim N, de Lima Alves F, Rappsilber J, Klein PS, Jongens TA and Mourelatos Z (2010) Arginine methylation of vasa protein is conserved across phyla. *J Biol Chem* **285**, 8148–8154.
61 Lim AK, Tao L and Kai T (2009) piRNAs mediate posttranscriptional retroelement silencing and localization to pi-bodies in the *Drosophila* germline. *J Cell Biol* **186**, 333–342.

Supporting information

Additional Supporting Information may be found online in the supporting information tab for this article:
Fig. S1. A representative gel image showing the purity of the Me31B-GFP protein IP.
Table S1. Proteins identified in Me31B complexes using *in vivo* crosslinking.
Fig. S2. Uncropped Fig. 5D western blot image.